Working Memory Guides Perceptual Decisions Through Fast Capture and Slow Drift

Hyung-Bum Park[1] Weiwei Zhang[2]

[1] Department of Neuroscience, Washington University in St. Louis

[2] Department of Psychology, University of California, Riverside

Abstract

The top-down influence of working memory (WM) can manifest as both attentional capture and small systematic biases in perceptual judgement (i.e., “tinted lens” effect). Yet it remains unclear whether these influences arise from a single mechanism or reflect functionally distinct processes operating over different timescales. Across two experiments, we embedded a perceptual estimation task during the delay interval of a WM task and tracked continuous mouse trajectories during both perceptual matching and subsequent WM tests. Hierarchical Bayesian mixture modeling revealed robust bidirectional attraction between memory and perception. Time-resolved analyses of mouse trajectories further revealed two distinct components: an early, endpoint-inconsistent deviation that varied with movement onset latency, whereas a slower, endpoint-consistent drift that closely tracked biases in the final report. This pattern is consistent with a fast, capture-like influence of the WM template, and a sustained bias in the evolving decision, respectively. Notably, the prospective influence of WM on perception expressed both early deviation and sustained drift, whereas the retrospective influence of perception on WM primarily involved the sustained component. These findings indicate that WM shapes perceptual decisions through at least two temporally distinct contributions, and illustrate how continuous trajectories can reveal the dynamic structure of top-down influences within single trials.

Keywords: working memory, perceptual appearance, attentional capture, mouse tracking, cognitive penetrability

Statement of Relevance

Our minds do not simply record the external world as it is, but reconstruct it actively through the lens of past experience and internal goals. Using continuous mouse-tracking, this study shows that working memory (WM) influences what we attend to and what we see, yet these effects unfold over different timescales. WM can momentarily capture attention toward memory-matching information while also producing a slower, sustained shift that changes how things appear. These findings suggest that WM serves as an active and flexible prior that continuously integrates past and present in shaping perceptual experience.

Working memory (WM) is a core cognitive system for maintaining task-relevant information and for preparing the perceptual system to interact with upcoming input (Cowan, 2001; Nobre & Stokes, 2019). Rather than functioning solely as a short-term storage, WM dynamically configures processing priorities by pre-activating feature-selective neural codes, thereby linking prior knowledge and current perceptual decisions within a predictive control framework (Myers et al., 2017; Summerfield & de Lange, 2014). In this view, WM provides an internal context that shapes how sensory evidence is sampled, weighted, and integrated over time.

This top-down influence manifests through at least two fundamental mechanisms. First, the features instantiated in WM can serve as an attentional template that biases selection toward matching inputs through competitive selection (Desimone & Duncan, 1995; Wolfe, 1994). Behaviorally, this often appears as attentional capture, wherein attention is automatically drawn toward WM-matching input even when such capture conflicts with current task demands (Olivers et al., 2006; Soto et al., 2008; Park & Zhang, 2024; Won & Zhang, 2025). Second, and more controversially, WM may directly alter how features appear perceptually, functioning as a "tinted lens" that pulls new sensory information toward remembered features (Teng & Kravitz, 2019; Teng et al., 2023). This tinted-lens account posits that WM content can shift nearby sensory representations toward itself, producing reliable systematic distortions in perceived color, orientation, or shape. This theoretical framework aligns with sensory-recruitment theories proposing that sensory cortices contribute simultaneously to both perception and memory maintenance (Harrison & Tong, 2009; Serences et al., 2009; Rademaker et al., 2019), as well as attractor network models in which stable memory states act as attractor basins that bias the readout of sensory evidence (Burak & Fiete, 2009; Wimmer et al., 2014).

Historically, the two types of influences, *attentional capture* and *perceptual bias*, have been investigated as largely separate phenomena employing distinct methodological approaches, leaving open whether they reflect different stages of a single underlying mechanism, or reflect functionally and mechanistically distinct computational operations that unfold across different timescales. Answering these questions requires a method capable of tracking how WM influences perception continuously within a single trial. Conventional measures such as accuracy and reaction time are insufficient as they conflate early attentional events with later representational changes. Neurophysiological evidence demonstrates that WM's influence can indeed operate on multiple timescales. For example, event-related potential studies have documented that WM-matching items modulate early visual components (e.g., P1/N1, around 100–200 ms post-stimulus), consistent with rapid attentional modulation, as well as later components associated with conflict resolution and response mapping, which occur over 500 ms post-stimulus (Luck et al., 2000; Tan et al., 2014). These findings suggest the presence of temporarily distinct pathways, yet clear behavioral evidence isolating multiple WM-driven influences within the same perceptual decision has remained elusive.

The present study employs time-resolved mouse-tracking to examine how WM shapes perceptual decisions moment-by-moment. Continuous cursor trajectories provide a process-level readout of evolving choices and can reveal subtle early deviations as well as slower drifts that precede the final report (Park, 2025; Park & Zhang, 2024). This approach allows us to operationalize and dissociate two potential influences of WM. First, *attentional capture* manifest as an early, transient trajectory curvature toward the WM-matching feature that cannot be explained by the final endpoint response (Theeuwes et al., 2005). Second, *representational shift* manifests as sustained trajectory deviation, robust even after removing the transient early

deviations, which presumably drives the directional bias in the final response. To accomplish this, we adopted an analytic method to decompose the overall trajectory into two components, an early endpoint-inconsistent deviation and a sustained endpoint-consistent deviation (Park, 2025; see *Data Analysis* for detail).

Across two experiments, participants memorized a briefly presented sample color, performed a perceptual matching task embedded during the memory delay, and then completed a WM test. Experiment 1 examined how WM influenced ongoing perceptual decisions, and Experiment 2 examined the reciprocal influence of perceptual decisions and subsequent WM recall to investigate how the priority state of the maintained representation (i.e., prospective vs. retrospective influence) relates to early-versus-late components of the decision process. Across both experiments, we show that WM content can simultaneously capture spatial attention and bias perceptual appearance, but that these effects emerge on distinct temporal scales. Specifically, capture emerges and dissipates rapidly, reflecting transient priority-based competition, whereas bias develops gradually and persists throughout movement, reflecting sustained representational assimilation. Together, these findings reveal how distinct top-down signals from WM jointly shape visual experience in real time.

General Method

Participants

Thirty-three (19 female) and twenty-one (14 female) college students at the University of California, Riverside participated in Experiment 1 and 2, respectively, in exchange for course credit. Participants were aged between 18 and 24 years, reported normal or corrected-to-normal vision and normal color vision. Informed consent was obtained prior to participation, and all

experimental protocol was approved by the University of California, Riverside Institutional Review Board.

For Experiment 1, the target sample size was determined based on previous work adopting a closely related experimental and mouse-tracking procedure (Park & Zhang, 2024). A priori power analysis in G*Power 3.1 (Faul et al., 2007) for a two-tailed paired *t*-test with $\alpha = .05$ and a predicted effect size of $dz = 0.50$ indicated that 34 participants would provide approximately 80% power. The sample size for Experiment 2 was guided by the robust within-subject bias observed in Experiment 1 ($d = 1.29$), thus moderate *N*s are sufficient to detect reliable within-subject attraction effects. It should be noted that the primary statistical inferences in both experiments were based on hierarchical Bayesian modeling and resampling-based permutation tests (see *Data Analysis* for detail). The Bayesian analyses yielded decisive posterior credible intervals for the population-level parameter of key interest, and the permutation tests detected the predicted dissociation effects, supporting the adequacy of the sample size.

Stimuli and Procedure

Stimuli were presented on a 60 Hz LCD monitor calibrated with an X-Rite i1Pro spectrophotometer, with a grey background (15.1 cd/m²) at a viewing distance of 60 cm. Task procedures were identical in Experiments 1 and 2, except for a test array (Figure 1). Each trial began with central fixation (800 ms), followed by a sample display (100 ms) of a single colored square (1.6° × 1.6°), which appeared at one of four equally spaced locations on an imaginary circle (radius 4.3°) centered at fixation. The memory color was selected randomly from 180 evenly spaced hues on a circular CIELAB color space (Zhang & Luck, 2008).

After an unfilled 400-ms delay, the perceptual matching display appeared. A colored disk (1.6° diameter) replaced the central fixation point, surrounded by a continuous color-wheel

(radius 8.2°, thickness 2.2°) with 180 evenly distributed hues from the same color space. The target color for the perceptual matching task was offset by either 40° clockwise (CW) or counterclockwise (CCW) from the memorized color in the sample display. This relative offset was strategically chosen to fall within the similarity range that maximizes attraction in previous serial-dependence research (Fischer & Whitney, 2014). The target item remained visible until response, and participants reported the perceived hue of the target by moving the mouse cursor from the center of the screen to the best-matching color on the color-wheel with a click. Mouse trajectories (x and y coordinates and time relative to the cursor onset) were recorded continuously. Immediately after the click, 500 ms visual feedback appeared on the color-wheel, with a cross marking the color the participants picked and an arrow marking the target color. The color-wheel was randomly rotated on every trial to prevent fixed spatial mapping of the colors to locations on the wheel. The mouse cursor was re-positioned at fixation after the visual feedback.

Following another unfilled 500 ms delay, a test display occurred, which differed by experiment. Experiment 1 adopted a change-detection, in which the task array presented a single probe at the original memory item location, and participants indicated whether the probe matched or mismatched the remembered color by pressing one of two shoulder buttons on a gamepad (e.g., L1 for “no-change”, L2 for “change”). The participants used their dominant hand (right hand for all subjects) for the mouse clicking for the perceptual matching task and the nondominant hand for the change-detection task. Change and no-change trials occurred with equal probability. On change trials, the probe color rotated 60°, 120°, or 180° in either direction from the memory color with equal probability. Because the preceding perceptual matching target was always positioned 40° CW or CCW relative to the memory color, this systematic manipulation of change magnitude allowed us to test whether the perceptual judgment made

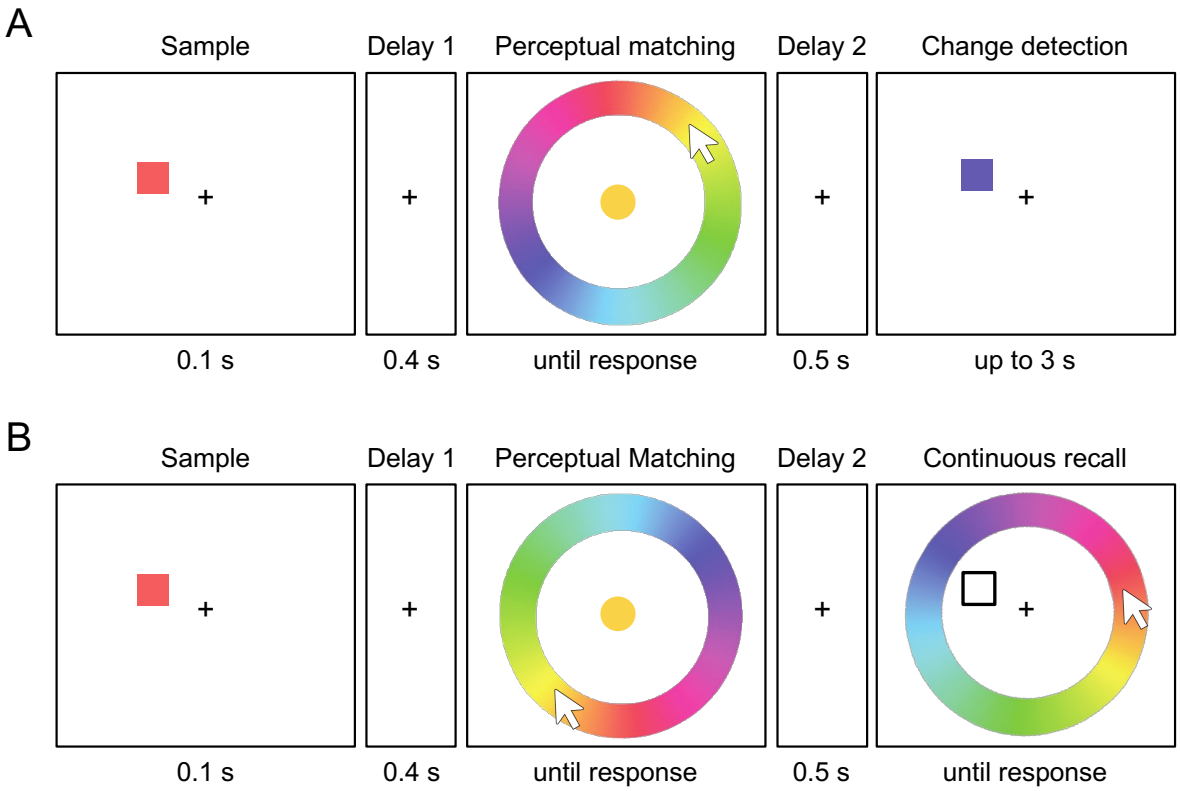

Figure 1. Task procedure for Experiment 1 (A) and Experiment 2 (B). (A) Experiment 1 embedded a perceptual matching task within the delay interval of a working memory (WM) change-detection task. After viewing a sample color and a short delay, participants reported the color of a continuously visible target using a color-wheel (perceptual matching), followed by a second delay and a change-detection, where change magnitude varied at every 60° in both directions (−180°:60°:180°). (B) Experiment 2 combined perceptual matching with continuous WM recall. After the sample and delay, participants performed a perceptual matching report, followed by a second delay and a continuous recall of the memorized color using a color-wheel.

during WM maintenance influenced the subsequent representation of the memory item. Auditory feedback followed each response, consisting of a 500 ms low-pitch tone for correct answers and a high-pitch tone for errors.

Experiment 2 adopted a continuous recall paradigm, in which the test display consisted of an outlined square at the original location of the memory item and another color-wheel that had a circular rotation to random degrees in order to prevent a strategical mapping of stimulus to color-wheel location during the previous perceptual matching task. Participants reproduced the

remembered color by moving the mouse cursor away from the center of the screen and then clicking the best-matching color on the wheel. Immediate feedback was provided in the same manner as that for the perceptual matching task. In both experiments, the mouse cursor was automatically re-centered at fixation after each click, and all participant completed 300 trials in total, divided into three blocks with brief breaks.

Data Analysis

Data and code availability. All primary and processed data, as well as custom analysis codes, are publicly available via the Open Science Framework repository (https://osf.io/3pyjh).

Hierarchical Bayesian Mixture Modeling

Perceptual matching error in Experiment 1 and 2 was defined as the signed angular distance in degrees between each reported color and the corresponding physical target color in the perceptual matching task. Similarly, memory recall error was defined as the signed angular distance in degrees between the reported and the original memory colors during WM recall in Experiment 2. These errors were modeled with a hierarchical Bayesian mixture model that extends the standard continuous estimation framework (Zhang & Luck, 2008; Park & Zhang, 2024). The model is expressed as a mixture of two distributions representing whether recall responses are based on noisy target representation or non-informative guesses (Figure 2). Specifically, the von Mises component captures responses based on noisy feature representations with mean (μ) that indexes inaccuracy or bias and concentration κ that indexes precision (reported as imprecision σ converted from κ). The uniform component captures guesses or lapses with mixture weight g, the height of the uniform probability distribution. Although guessing was expected to nearly minimal in the perceptual matching task since the target remained visible until response, the same modeling approach was applied to both perceptual matching and continuous

WM recall errors in Experiment 2. This modeling approach permits a principled cross-task comparison of bias magnitude while accounting for occasional lapses or memory failures.

The bias effects in serial-dependence and WM are typically reliable but numerically small, often about a few degrees (Barbosa & Compte, 2020; Park, 2025). Hierarchical Bayesian modeling offers key advantages for this context, because it simultaneously accounts for multiple sources of variability (e.g., across participants, conditions, and trials), thereby stabilizing estimation of small effects (Oberauer et al., 2017; see also Frischkorn & Popov, 2025). This approach allows noisy parameter estimates to be shrunk toward the population mean, leading to more robust and reliable results (Shiffrin et al., 2008). The choice of reasonably informative to non-informative priors was determined following previous studies with similar modeling approach (Oberauer et al., 2017; Park & Zhang, 2024). We took a total of 4,000 samples after 4,000 warm-ups with four chains of Markov chain Monte Carlo sampling. It yielded posterior matrices of population-level parameters sized, for example, 12,000 (samples) × 33 (subjects) × 2 (conditions) for Experiment 1. Convergence was assessed using the Gelman-Rubin $\hat{R}$ statistic, with all population-level parameters showing values equal or close to 1.0 (Gelman & Rubin, 1992). Statistical inferences are reported in terms of posterior means and the 95% highest density credible intervals ($HDI_{95\%}$; Kruschke, 2015).

Mouse Trajectory

Mouse cursor trajectories were recorded continuously from stimulus onset until the click on the color-wheel during both the perceptual matching task (Experiments 1 and 2) and the subsequent WM recall task (Experiment 2). Movement onset was defined as the first sample in which the cursor moved more than five pixels from the central starting position. To compare trajectories across trials and participants, each trajectory was time-normalized from movement

onset (0%) to the final response (100%). On average, participants initiated the cursor movement at about 25.7% [$CI_{95\%}$: 22.6%, 28.8%] of the normalized time scale.

To place all trials in a common spatial reference frame, each trajectory was rotated so that the true target color mapped to the top of the response color-wheel with Cartesian coordinate (0, r), where r is the wheel radius. This normalization ensured that any horizontal deviation directly reflects attraction toward or repulsion away from the WM-matching color during perceptual matching, or relative to the intervening perceptual target during WM recall.

The direction and magnitude of trajectory curvature were summarized as the signed area under the curve (AUC), computed as the integral of horizontal cursor offsets across the normalized time axis. After confirming that there was no reliable difference in curvature magnitude between trials where the perceptual target lay clockwise (CW) or counterclockwise (CCW) of the WM item, $t(32) = 0.08$, $p = .933$, Cohen's $d = 0.01$, we flipped the sign for the CW trials. Consequently, positive AUC values for perceptual matching indicate attraction toward the WM representation, and negative AUCs for WM recall in Experiment 2 indicate attraction toward the earlier perceptual decision.

To distinguish transient attentional capture from the more sustained, endpoint-consistent bias, we employed a decomposition method utilizing an endpoint-bias correction (Park & Zhang, 2022). For each trial, we computed a reference path by directly connecting the starting point at fixation to the final clicking point on the wheel, while preserving the same radial progress over time. Subtracting this reference path from the overall trajectory yielded trajectory deviations for the *capture* component that cannot be explained by the endpoint. The complementary *shift* component was defined as the residual (i.e., overall trajectory = capture + shift) and indexes the

portion of curvature that is geometrically consistent with the endpoint displacement. The overall AUC is thus the sum of capture ($AUC_{capture}$) and shift (AUC_{shift}).

Because AUC_{shift}, by construction, reflects curvature aligned with the chosen endpoint, its magnitude is expected to covary with the final response bias. Accordingly, we do not treat AUC_{shift} as a statistically independent source of evidence about the final report. Instead, the decomposition serves as a variance-partitioning tool that provides a principled way to test whether different portions of the trajectory associate with theoretically relevant predictors, such as movement initiation latency or final judgment bias, in ways that would functionally dissociating WM's top-down influences. This approach mirrors prior decomposition strategies in serial dependence and dynamic decision-making research, where early deviations and late drifts reflect separable computational influences on evolving choices, even in the opposite directions (e.g., early repulsion vs. later attraction; Park, 2025).

Beyond area-based point estimates, we further conducted time-resolved analysis using a recently developed destination-vector transformation (DVT) to capture moment-by-moment dynamics of decision making (Park & Zhang, 2024; Figure 5A). Rather than focusing on the instantaneous cursor position, DVT estimates the projected location on the continuous response scale at each time point, based on the direction of the local movement vector connecting two consecutive samples. For a trajectory with n samples, DVT produces $n-1$ destination-vectors in circular degrees, providing a time series of "intended destinations". We applied DVT separately to the overall, capture, and shift trajectories, and averaged the resulting time series across trials and participants to measure the temporal dynamics of how WM or recent perceptual input shaped the evolving response tendencies. Time-resolved differences between conditions and components

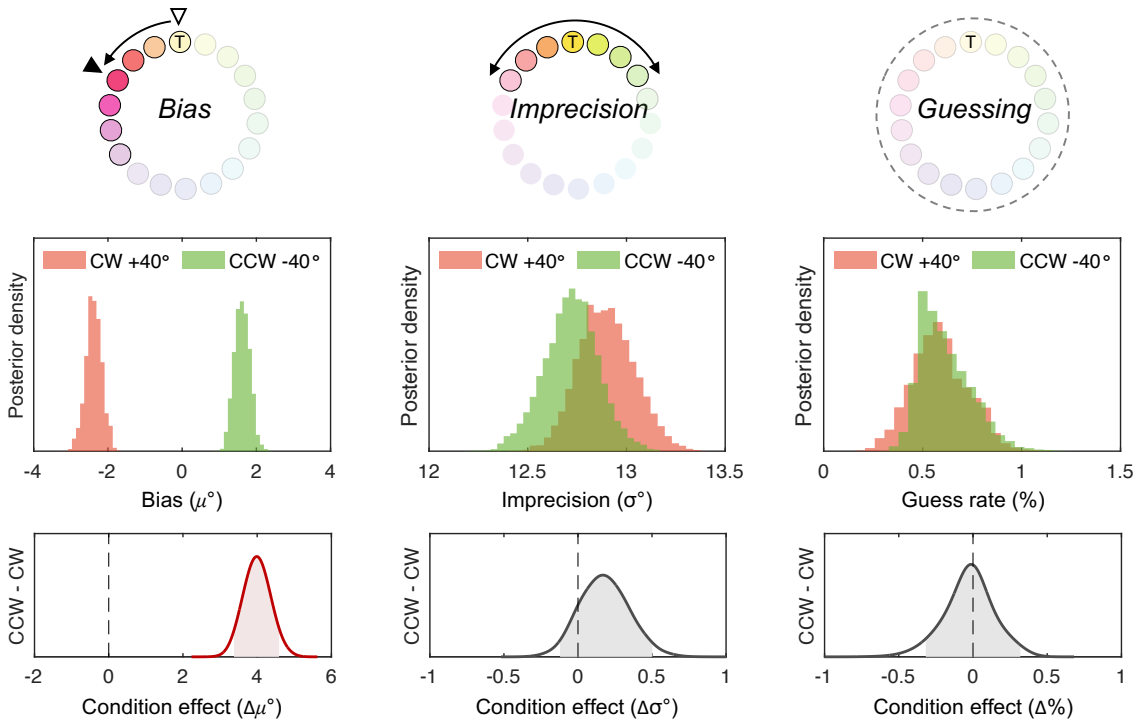

Figure 2. Hierarchical Bayesian parameter estimates for Experiment 1. Posterior distributions of the Mixture model population-level parameters are shown separately for CW (+40°) and CCW (−40°) conditions for bias (μ), imprecision (σ), and guess rate (g). The lower panels show posterior distributions of condition effects (CCW − CW) for each parameter. A credible condition difference was observed for bias (Δμ), with 95% highest density intervals ($HDI_{95\%}$) beyond zero. Shaded areas represent $HDI_{95\%}$.

were evaluated using within-subject cluster-based permutation tests (10,000 label swaps), providing a robust assessment of temporal intervals in which the components diverged.

Results

Experiment 1: Perceptual Matching

Endpoint Bias Toward Working Memory

Perceptual matching errors as the endpoint of the mouse trajectory showed the predicted attraction toward the WM-matching color on the response color-wheel. Mean circular error was negative in the CW condition (i.e., the perceptual target color is CW to the memory item; M = −2.44° [$CI_{95\%}$: −3.03°, −1.85°]) and positive in the CCW condition (+1.89° [$CI_{95\%}$: +1.09°,

+2.68°]), yielding a reliable difference between conditions, $t(32) = -7.31$, $p < .001$, Cohen's $d = -1.29$. A Hierarchical Bayesian Mixture model confirmed these attraction effects (Figure 2). Posterior distributions of the population-level bias (μ) parameter were in opposite directions for CW and CCW trials, and their contrast credible excluded zero, $\Delta\mu_{CCW-CW} = +4.00°$ [$HDI_{95\%}$: +3.37°, +4.59°], indicating robust attraction toward the WM color. Imprecision (σ) and guess rate (g) did not differ credibly between CW and CCW trials ($\Delta\sigma = 0.18°$ [$HDI_{95\%}$: −0.12°, 0.50°]; $\Delta g = -0.03\%$ [$HDI_{95\%}$: −0.32%, 0.32%]).

Mouse Trajectory Deviation Toward Working Memory

Next we assess the entire mouse trajectory beyond the endpoint to reveal the temporal dynamics of the retrieval and decision process. The overall trajectory for both CW and CCW trials showed a clear early deviation toward the WM color, which peaked soon after movement onset and declined as the movement progressed (Figure 3a), which manifested as the sizable horizontal deviations (Figure 3b) and the $AUC_{overall}$ (Figure 3c, 13.8 px [$CI_{95\%}$: 10.9 px, 16.8 px]), $t(32) = 9.28$, $p < .001$, Cohen's $d = 1.64$). Moreover, $AUC_{overall}$ scaled with how fast participants initiated mouse cursor movement upon perceptual target onset. A within-subject median-split on movement onset latency revealed larger deviations on early-onset trials (AUC_{early} = 24.1 px [$CI_{95\%}$: 20.0 px, 28.2 px]), than on late-onset trials (AUC_{late} = 9.6 px [$CI_{95\%}$: 6.8 px, 12.3 px]), $t(32) = 8.05$, $p < .001$, Cohen's $d = 1.42$. This speed contingency suggests that rapid movements are subject to a brief capture toward the WM-matching item, thereby magnifying overall trajectory curvature. In contrast, critically, movement onset latency did not influence the final perceptual errors which showed a nonsignificant difference between early-onset trials (2.32° [$CI_{95\%}$: 1.64°, 3.00°] and late-onset trials (1.88° [$CI_{95\%}$: 1.21°, 2.55°]) did, $t(32) = 1.23$, $p = .229$, Cohen's $d = 0.22$. This null effect rules out the possibility that endpoint

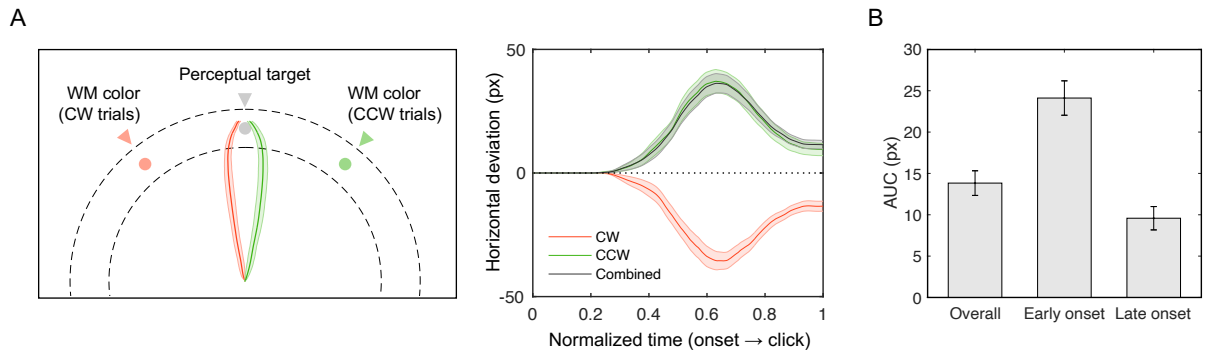

Figure 3. Mouse-tracking evidence for WM-induced perceptual bias in Experiment 1. (A) Average trajectory paths (left) and average horizontal trajectories (right), plotted separately for CW (+40°) and CCW (−40°) conditions. Shaded bands indicate 95% confidence intervals. (B) Area-under-the-curve (AUC) analyses of trajectory curvature. Early and late onset represent trials median split of movement onset latency. Error bars standard errors of the mean.

bias merely reflects any under-corrected motor deviation from initial capture, and instead suggests a genuine shift in perceptual appearance. Because $AUC_{overall}$ conflates these influences, it is essential to decompose the measure to isolate the distinct contributions of attention capture and appearance change.

Mechanistic Dissociation: Capture versus Shift

To determine whether earlier, endpoint-inconsistent deviations and later, endpoint-consistent drifts show different functional relationships with behavioral predictors, overall curvature was decomposed with an endpoint-bias correction (Figure 4A). For each trial, a reference line connecting the start and endpoint was subtracted from the observed path, yielding the *capture* component (deviations not explained by the endpoint). The *shift* component was defined as the residual (i.e., overall = capture + shift). We computed AUC for each component and conducted a set of individual-differences tests relating these components to movement onset latency and to the magnitude of the final perceptual shift.

This decomposition revealed distinct prediction patterns across the two components (Figure 4D). Movement onset latency reliably predicted $AUC_{capture}$, $r(31) = -.59$ [$CI_{95\%}$: −.77,

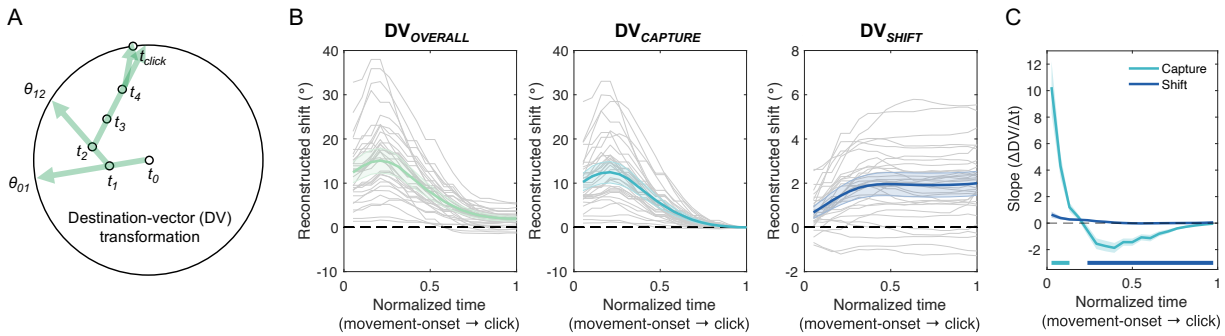

Figure 4. Destination-vector transformation and decomposition analyses in Experiment 1. (A) Schematic illustration of the destination-vector (DV) transformation method, which represents each movement segment as an angle (θ) relative to the target based on two consecutive moment points, allowing reconstruction of intended feature values across time (Park & Zhang, 2024). (B) Reconstructed DV dynamics for overall deviation (green), capture (cyan), and shift (blue). Thin gray lines show individual participant DV series and thick lines with shaded bands indicate group means and 95% confidence intervals. (C) Slope differences between capture and shift DV series. Capture showed a steeper early slope, whereas shift dominated later in the movement. Colored horizontal bars denote time windows with significant cluster-based permutation effects ($p < .05$).

−.30], $p < .001$, such that faster initiations were associated with larger endpoint-inconsistent deviations, whereas it showed little relationship with AUC_{shift}, $r(31) = -.08$ [$CI_{95\%}$: −.41, .27], $p = .654$. In contrast, the magnitude of the final endpoint bias was strongly associated with AUC_{shift}, as expected given that it is defined with respect to the endpoint path, $r(31) = .86$ [$CI_{95\%}$: .74, .93], $p < .001$, but was weakly related to the $AUC_{capture}$, $r(31) = .17$ [$CI_{95\%}$: −.18, .49], $p = .336$. Once endpoint-consistent curvature was factored out, the remaining capture-only component showed a selective relationship with movement onset latency and minimal association with the final perceptual bias. This pattern suggests that $AUC_{capture}$ tracks an early, initiation-linked influence of working memory that is functionally distinct from the endpoint-consistent bias reflected in AUC_{shift}.

Time-Resolved Decision Dynamics: Destination-Vector Series

The analyses of movement latency and component dissociation suggested that WM influences manifest as both transient attention capture and sustained representational shift. To

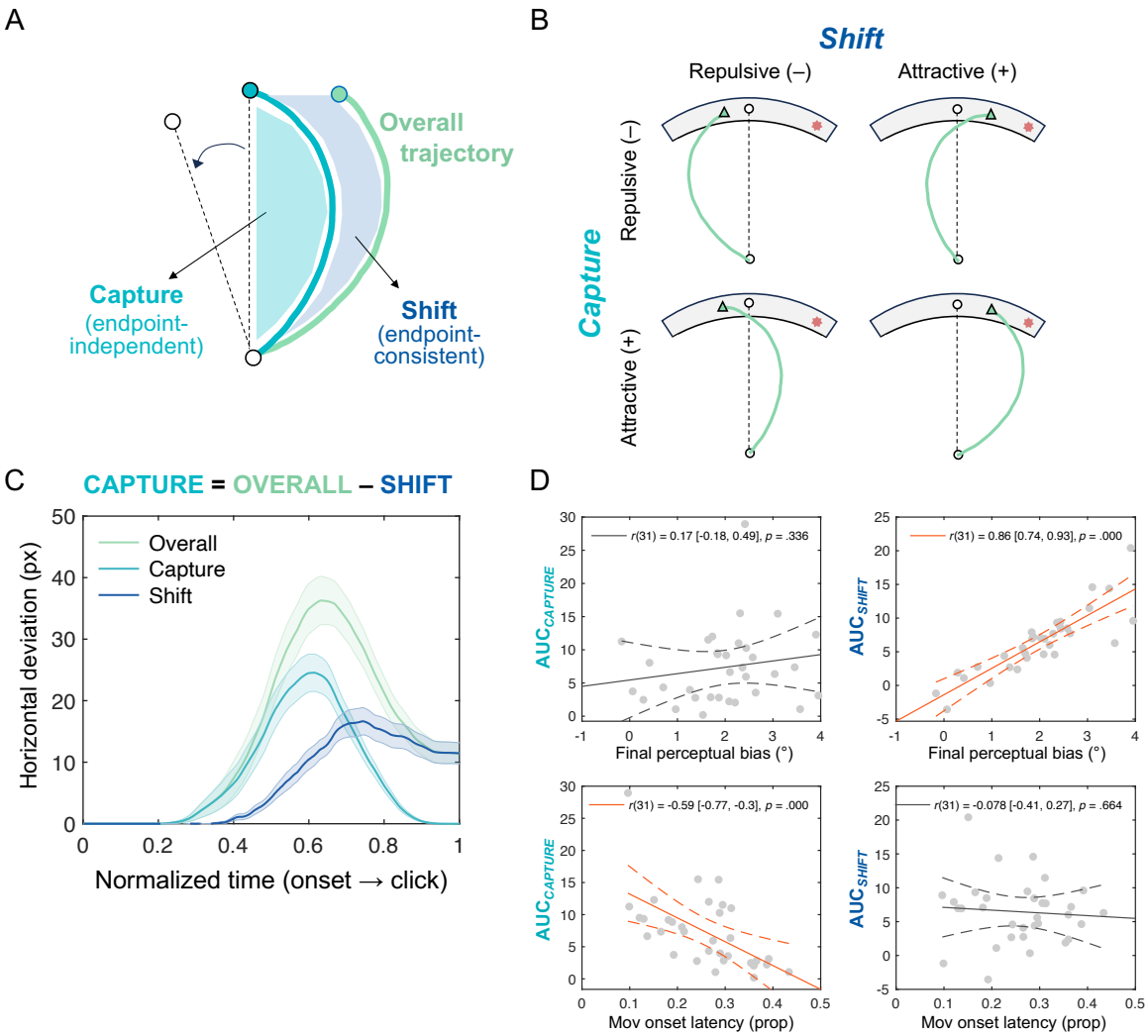

Figure 5. Decomposition of trajectory bias into capture and shift components in Experiment 1. (A) Schematic illustration of the endpoint-based decomposition. The observed overall trajectory (green) is expressed as the sum of an endpoint-inconsistent capture component (cyan) and an endpoint-consistent shift component (blue). (B) Conceptual examples that capture and shift can manifest as independent attractive (positive) or repulsive (negative) deviations from the source of bias (red markers). White circles and green triangles indicate the true target location and the judgment endpoint, respectively. (C) Average time course of horizontal deviation for the overall, capture, and shift trajectories, time-normalized from movement onset to the final click. Shaded bands indicate 95% confidence intervals ($CI_{95\%}$). (D) Correlations of area-under-the-curve (AUC) measures for capture and shift with final perceptual bias (top row) and movement onset latency (bottom row). Solid lines show the best linear fit and dashed lines the $CI_{95\%}$, with red lines indicating statistically significant effects.

track how these influences unfolded over time, we used DVT to reconstruct the latent decision variables throughout the movement trajectory (Figure 5A). The decomposition (Figure 5B)

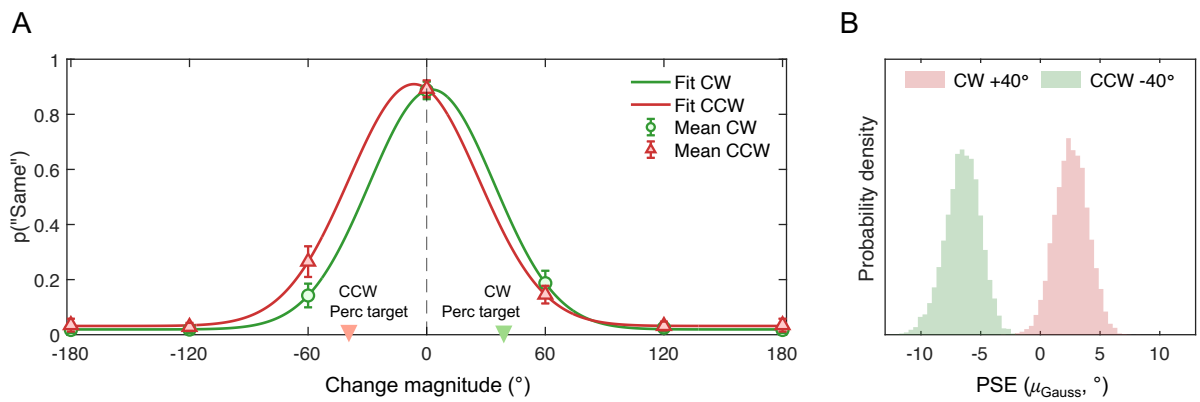

Figure 6. Working memory change-detection performance in Experiment 1. (A) Proportion of "same" responses as a function of change magnitude, with Gaussian fit curves (solid lines) shown separately for CW (+40°) and CCW (−40°) trials. Markers with error bars indicate group means and 95% confidence intervals. Inverted triangles along the x-axis denote the corresponding locations of the preceded perceptual target features. (B) Posterior distributions of the point of subjective equality (PSE, μ_{Gauss}) estimated separately for CW and CCW conditions.

mirrored the AUC findings. The capture time series ($DV_{CAPTURE}$) rose sharply at movement onset and returned toward baseline before the response was completed, consistent with transient attentional capture. The shift component (DV_{SHIFT}) remained positive throughout the trajectory, emerging early and persisting until the response, consistent with a steady representational shift.

To directly compare these temporal dynamics, we examined slope differences between the capture and shift effects. Cluster-based permutation testing (10,000 iterations) revealed an early interval (5% to 15% normalized time) where capture increased more steeply than shift (i.e., capture slope > shift slope, $p_{cluster} < .05$), followed by a late period (25% to 95% normalized time) where the difference reversed in sign (i.e., capture slope < shift slope, $p_{cluster} < .05$; Figure 5C). These results indicate that WM exerts dissociable influences on decision dynamics. A rapid capture process dominates early in the movement and a slower, sustained shift persists throughout and aligns with the endpoint bias.

Experiment 1: Working Memory Change Detection

The WM change-detection task involved systematic manipulations of change magnitude, varying memory-to-probe color offset every 60° steps. To test whether perceptual matching influenced WM content retrospectively, we modeled the psychometric function relating the probability of "same" responses as a function of change magnitude, where 0° represents no-change trials (Figure 6A). The group-aggregated curves were fit with the Gaussian function to estimate the point of subjective equality (PSE, μ_{Gauss}), slope (σ), amplitude (*Amp*), and *lapse* rate, separately for CW and CCW curves. This revealed a reliable shift of the PSE (μ_{Gauss}) between CW (+2.59°) and CCW (−6.48°) conditions. For statistical inference, subject-level bootstrap resampling (10,000 iterations) provided $CI_{95\%}$ and two-sided p values for the differences in these estimates across the conditions. The PSE (μ_{Gauss}) showed a reliable condition difference between the CW and CCW condition (9.11° [$CI_{95\%}$: 4.67°, 13.42°], $p_{boot} < .001$). None of other parameters showed reliable differences (for *Amp*, −0.01 [$CI_{95\%}$: -0.03, 0.02], $p_{boot} = .529$; for σ, −1.25° [$CI_{95\%}$: −4.12°, 1.68°], $p_{boot} = .384$; for *lapse*, −0.012 [$CI_{95\%}$: −0.026, 0.001], $p_{boot} = .071$).

The change-detection results demonstrate that WM judgments are reliably biased in the direction of the preceding perceptual decision. Experiment 2 replaced a binary change-detection with a continuous WM recall procedure following the perceptual matching task (Figure 1B), allowing a direct comparison between attraction observed during perceptual matching and that during mnemonic recall.

Experiment 2

Endpoint Bias between Perceptual Matching and Working Memory

Hierarchical Bayesian Mixture modeling of continuous-report errors provided converging evidence for reciprocal attraction between WM and perception (Figure 7). Posterior distributions of the μ parameter revealed opposite biases across the responses. During perceptual matching, μ

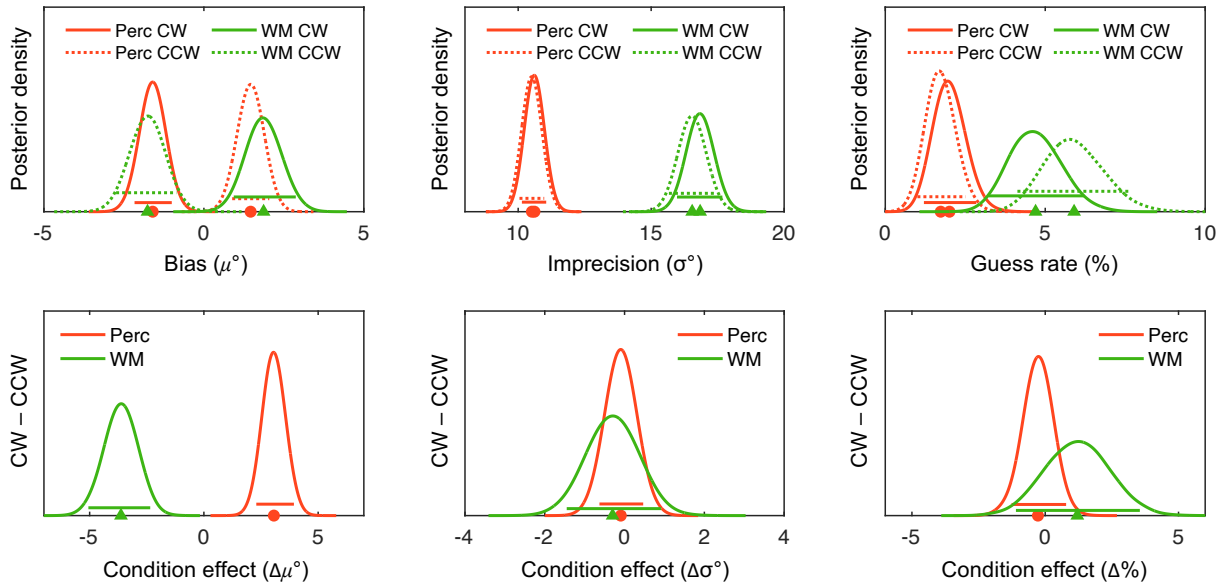

Figure 7. Hierarchical Bayesian Mixture modeling of continuous-report errors in Experiment 2. (Top row) Posterior distributions of population-level parameters for perceptual matching (Perc; red) and working memory recall (WM; green), shown separately for clockwise (CW; solid lines) and counterclockwise (CCW; dotted lines) conditions. (Bottom row) Posterior distributions of condition effects (CW − CCW) for each parameter. Markers and horizontal bars along the x-axis represent posterior means and 95% highest density intervals, respectively.

shifted toward the WM color, replicating Experiment 1 ($\Delta\mu_{CCW-CW}$ = 3.06° [$HDI_{95\%}$: 2.29°, 3.94°]). Critically, during subsequent WM recall, μ shifted in the opposite direction, toward the just-seen perceptual target ($\Delta\mu_{CCW-CW}$ = −3.63° [$HDI_{95\%}$: −5.06°, −2.34°]). Although opposite in sign, their absolute magnitudes were similar, indicating reciprocal influences of comparable strength. By contrast, imprecision (σ) did not differ credibly between CW and CCW trials in either phase (perceptual matching: $\Delta\sigma$ = −0.10° [$HDI_{95\%}$: −0.63°, 0.47°]; WM recall: $\Delta\sigma$ = −0.30° [$HDI_{95\%}$: −1.46°, 0.92°]). Guess rate (g) also remained low and stable (perceptual matching: Δg = −0.27% [$HDI_{95\%}$: −1.27%, 0.79%]; WM recall: Δg = 1.20% [$HDI_{95\%}$: −1.11%, 3.55%]). These results show that WM and perceptual judgments mutually biased one another with comparable magnitudes but in opposite directions, extending the WM-to-perception effect in Experiment 1 to the complementary perception-to-WM influence.

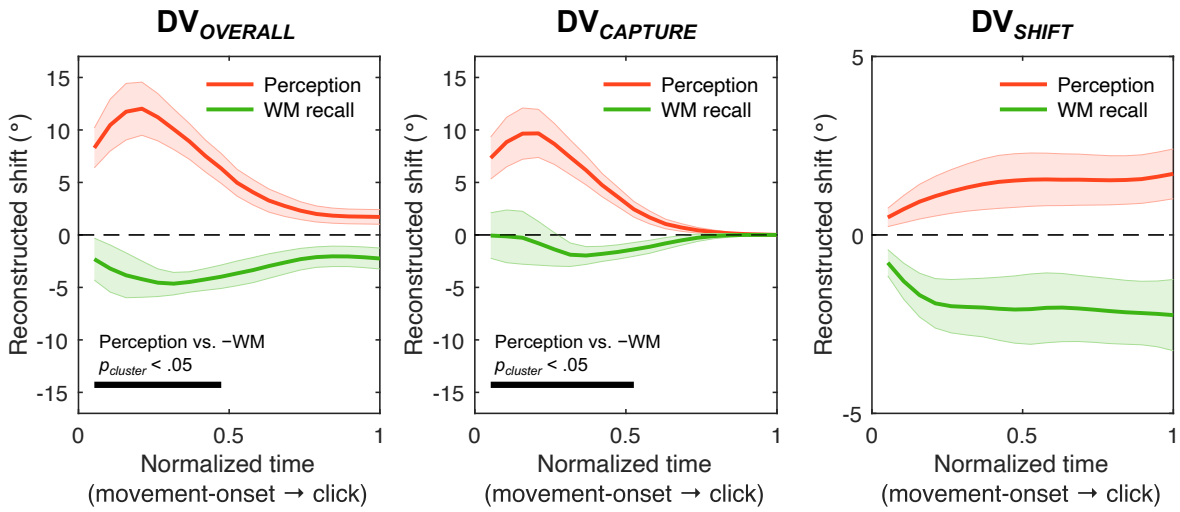

Figure 8. Reconstructed destination-vector (DV) dynamics and decomposition analyses in Experiment 2. Mean DV series with 95% confidence intervals over normalized time for perceptual matching (Perception; red) and working memory (WM) recall (green), shown separately for $DV_{OVERALL}$, $DV_{CAPTURE}$, and DV_{SHIFT} (left to right). Black horizontal bars indicate time intervals with significant cluster-based permutation effects contrasting perceptual matching and sign-flipped WM recall ($p < .05$).

Time-Resolved Decision Dynamics: Destination-Vector Series

To examine how bidirectional biases unfolded during movement, we applied the DVT to mouse trajectories for perceptual matching and WM recall, and decomposed them into the capture ($DV_{CAPTURE}$) and shift (DV_{SHIFT}) components that showed dissociable temporal dynamics for the two responses (Figure 8). Perceptual matching showed strong early deviations toward the WM color, whereas WM recall exhibited minimal early curvature. This asymmetry was primarily attributed to the capture component ($DV_{CAPTURE}$). During perceptual matching, capture rose steeply after the movement onset and declined thereafter, whereas in WM recall it was effectively minimal. In contrast, the shift component (DV_{SHIFT}) showed steadily increasing amplitude across time, but with opposite directions for the two responses that mirrors the endpoint bias.

Cluster-based permutation tests (10,000 label-swaps within subject) on the reconstructed destination-vectors confirmed this dissociation. This analysis identified a reliable early interval for capture in which perceptual matching exceeded WM recall, spanning from 5% to 55% of normalized time from movement onset to final click ($p_{\text{cluster}} < .05$), consistent with capture being expressed only during perceptual matching. For shift, no clusters survived correction (all $p_{\text{cluster}} > .05$), indicating comparable sustained bias across phases.

Together, these results demonstrate the reciprocal but asymmetrical interactions between perceptual matching and WM recall. Specifically, perceptual matching engages both capture and shift dynamics, whereas WM recall primarily shows a sustained shift, with little capture by the previous perceptual input. This dissociation suggests that WM-based attention capture for perceptual matching may likely result from the prioritization of WM contents (e.g., for maintenance and protection from interference by incoming perceptual inputs).

General Discussion

The present study examined how WM shapes perceptual judgements in relation to its established role in guiding attentional selection (see Table 1). Across two experiments, we observed bidirectional attraction effects between WM and perception. Perceptual judgments were systematically biased toward the feature value held in WM, and subsequent WM recall showed bias toward the preceding perceptual decision. These findings provide time-resolved behavioral evidence that WM's top-down influence is not well captured by a single, unitary process. Instead, the dynamics of mouse trajectories suggest that at least two dissociable components. Specifically, an early, transient influence emerges shortly after movement initiation, whereas a later, more sustained influence persists throughout the appearance judgement.

Three converging findings support this conclusion. First, decomposing trajectories into endpoint-inconsistent and endpoint-consistent curvature revealed distinct relationships with movement onset latency and final estimation bias. The early, transient curvature (capture) was selectively correlated with how quickly a response was initiated but not with the final bias. In contrast, the endpoint-consistent curvature (shift) closely tracked the magnitude and direction of the final report, as expected given that it is defined relative to the endpoint path, but was not strongly related to response initiation speed. Second, time-resolved destination-vectors analyses confirmed distinct temporal profiles. The capture component peaked sharply near movement onset and quickly dissipated, whereas the shift component emerged more gradually and remained elevated until the response was completed[1]. Third, and most importantly, the expression of these two components was functionally distinct across directions of influence. When WM prospectively influenced perception, both capture and shift were evident. When perception reciprocally influenced WM, only a sustained shift was evident, with minimal evidence for robust early capture-like curvature. This asymmetry implies different underlying mechanisms for prospective and retrospective interaction.

The fast-acting capture component can be understood as a behavioral signature of attentional guidance. It reflects a transient top-down priority signal that WM generates to bias competition toward matching features. This interpretation aligns with the biased competition model, which posits that active WM representations pre-activate corresponding feature-selective neural populations, granting a competitive advantage to matching sensory input for selection

[1] Note that these temporal profiles are not a trivial consequence of the decomposition procedure. Although the shift component is defined with respect to the final response endpoint, this constraint only anchors the late portion of its destination-vector time series. Earlier values can in principle remain near zero, reverse in sign, or fluctuate. The fact that DV_{SHIFT} tends to emerge gradually and remain elevated throughout the movement therefore reflects a genuine regularity in the trajectory dynamics, rather than a pattern that is mathematically inherited from the endpoint correction itself.

(Desimone & Duncan, 1995; Serences & Yantis, 2006). The initial deviation of the cursor toward the WM-matching color follows naturally from this early priority signal as the system momentarily resolves competition between the target and the memory-matching feature value. The transient rise and subsequent correction are consistent with models in which attention can be briefly captured by a salient or goal-relevant item but then disengaged to reorient toward the primary task goal (Dieciuc et al., 2019). Continuous trajectory analysis thus provides a process-level window into how this capture-and-disengage sequence unfolds within a single decision.

The pattern observed in Experiment 2 further clarifies the conditions under which this early capture-like curvature is expressed. Capture was evident when the WM representation served a prospective role as an attentional template for the upcoming perceptual decision, but it was effectively minimal when the influence was from a just-encoded percept back onto memory (Park et al., 2017). This suggests that capture is not an automatic consequence of holding any mnemonic representation, but reflects the priority state of WM when it is actively used to guide upcoming behavior (Park & Zhang, 2024). Neuroimaging studies support this distinction, showing that prospective WM templates engage frontoparietal networks that broadcast priority signals to sensory areas, whereas retrospective maintenance primarily involves sensory reinstatement without prioritization (Myers et al., 2017; van Loon et al., 2018). In this sense, a WM template that is actively guiding behavior is functionally distinct from a more passive trace of a previous percept, and the former is more likely to produce the rapid priority signal that manifests as transient motor capture toward memory-matching input.

The broader pattern of results fits naturally within a precision-weighted integration framework, in which perceptual readout combines current sensory evidence with state-dependent priors supplied by WM. The similar magnitudes of the reciprocal endpoint biases in Experiment

2 argue against a purely task-specific artifact and instead support a general tendency for perceptual and mnemonic decisions to assimilate toward one another. The dissociation between the two trajectory components strengthens this interpretation, as early capture covaried with movement initiation latency but not endpoint bias, whereas sustained, endpoint-consistent curvature tracked endpoint bias independently of movement initiation latency. A single, undifferentiated decisional or motor account would predict shared variance across these measures and can therefore be ruled out. Instead, the data point toward multiple stages at which WM can influence evolving decisions, from early competition between candidate responses to later integration of mnemonic and sensory information.

What do these findings imply about whether the locus of WM's top-down influence is perceptual versus post-perceptual? A central challenge in debates over cognitive penetrability is distinguishing genuine perceptual changes from effects of attentional selection, decision rules, or response preparation (Firestone & Scholl, 2016). Our trajectory decomposition shows that WM-related biases are temporally extended and distinct from rapid capture, and that the sustained, endpoint-consistent component is closely aligned with the final report. These observations are compatible with frameworks in which WM acts as a prior that shapes late perceptual readout and/or decision formation, but they do not by themselves rule out a decisional locus. From a broader theoretical perspective, the current results support a state-dependent view in which memory contributes flexible priors for perceptual judgments. In this view, WM belongs to a broader class of mnemonic influences that configure perception and decision making through dynamic, context-dependent processing of environmental regularities (Girshick et al., 2011), semantic knowledge (Hansen et al., 2006; Bannert & Bartels, 2013), and episodic retrieval (Bosch et al., 2014; Won et al., 2023).

The integrative and gradual nature of the sustained bias aligns with predictive coding and Bayesian integration frameworks of perception (Ma et al., 2006; Knill & Richards, 1996). In these frameworks, perception arises from the ongoing integration of sensory evidence with top-down expectations. WM representations can be viewed as prior beliefs about which features are most likely to occur in the current context. The brain combines these priors with incoming sensory evidence (the likelihood) to form an updated estimate (the posterior) that is consequently biased toward the prior. Because this computation relies on evidence accumulation, it unfolds more slowly than the winner-take-all competition that characterizes early attentional selection. Within this framework, WM exerts at least two functionally distinct influences on perceptual decisions, one through competitive selection, and another through predictive integration, where mnemonic content acts as a prior that shapes perceptual inference.

In conclusion, this study demonstrates that WM functions both as a guide for attention and as a source of bias for perceptual decisions, with these roles supported by temporally distinct contributions to the unfolding decision process. A rapid priority signal produces brief capture when a template is prospectively relevant, while a slower assimilative process produces a gradual drift over the formation of a decision. Methodologically, by leveraging the temporal resolution of mouse-tracking and a variance-partitioning decomposition of trajectory deviations, the present approach offers a process-level view of decision dynamics that is sensitive to both transient and sustained influences within a single trial. The aligns with efforts to expand the rich behavioral repertoire for studying dynamic cognition (Nobre, 2022). More broadly, the findings support a view of cognition as a continuous synthesis of past and present, with WM acting as a goal-directed prior that shapes how sensory evidence is weighted over time. This dynamic interplay

allows perceptual decisions to balance stability with flexibility, supporting adaptive behavior in a changing environment (Kiyonaga et al., 2017).

Funding: This research was supported by the National Institute of Mental Health (1R01MH117132).

Conflicts of interest: All authors declare no conflicts of interest.

Ethics: This research was approved by the Institutional Review Board of the University of University of California, Riverside.

Data and code availability: All primary and processed data, as well as custom analysis codes, are publicly available via the Open Science Framework repository (https://osf.io/3pyjh).

Preregistration: No aspects of the study were preregistered

References

Bannert, M. M., & Bartels, A. (2013). Decoding the yellow of a gray banana. *Current Biology, 23*(22), 2268-2272.

Barbosa, J., & Compte, A. (2020). Build-up of serial dependence in color working memory. *Scientific Reports, 10*(1), 10959.

Bosch, S. E., Jehee, J. F., Fernández, G., & Doeller, C. F. (2014). Reinstatement of associative memories in early visual cortex is signaled by the hippocampus. *Journal of Neuroscience, 34*(22), 7493-7500.

van Loon, A. M., Olmos-Solis, K., Fahrenfort, J. J., & Olivers, C. N. (2018). Current and future goals are represented in opposite patterns in object-selective cortex. *eLife, 7*, e38677.

Burak, Y., & Fiete, I. R. (2009). Accurate path integration in continuous attractor network models of grid cells. *PLoS Computational Biology, 5*(2), e1000291.

Cowan, N. (2001). The magical number 4 in short-term memory: A reconsideration of mental storage capacity. *Behavioral and Brain Sciences, 24*(1), 87-114.

Desimone, R., & Duncan, J. (1995). Neural mechanisms of selective visual attention. *Annual Review of Neuroscience, 18*(1), 193-222.

Dieciuc, M. A., Roque, N. A., & Boot, W. R. (2019). The spatial dynamics of mouse-tracking reveal that attention capture is stimulus-driven rather than contingent upon top-down goals. *Journal of Experimental Psychology: Human Perception and Performance, 45*(10), 1285-1290.

Faul, F., Erdfelder, E., Buchner, A., & Lang, A. G. (2009). Statistical power analyses using G* Power 3.1: Tests for correlation and regression analyses. *Behavior Research Method, 41*(4), 1149-1160.

Firestone, C., & Scholl, B. J. (2016). Cognition does not affect perception: Evaluating the evidence for “top-down” effects. *Behavioral and Brain Sciences, 39*, e229.

Fischer, J., & Whitney, D. (2014). Serial dependence in visual perception. *Nature Neuroscience, 17*(5), 738-743.

Frischkorn, G. T., & Popov, V. (2025). A tutorial for estimating Bayesian hierarchical mixture models for visual working memory tasks: Introducing the Bayesian Measurement Modeling (bmm) package for R. *Behavior Research Methods, 57*(5), 144.

Gelman, A., & Rubin, D. B. (1992). Inference from iterative simulation using multiple sequences. *Statistical Science, 7*(4), 457-472.

van Loon, A. M., Olmos-Solis, K., Fahrenfort, J. J., & Olivers, C. N. (2018). Current and future goals are represented in opposite patterns in object-selective cortex. *eLife, 7*, e38677.

Hansen, T., Olkkonen, M., Walter, S., & Gegenfurtner, K. R. (2006). Memory modulates color appearance. *Nature Neuroscience, 9*(11), 1367-1368.

Harrison, S. A., & Tong, F. (2009). Decoding reveals the contents of visual working memory in early visual areas. *Nature, 458*(7238), 632-635.

Kiyonaga, A., Scimeca, J. M., Bliss, D. P., & Whitney, D. (2017). Serial dependence across perception, attention, and memory. *Trends in Cognitive Sciences, 21*(7), 493-497.

Knill, D. C., & Richards, W. (Eds.). (1996). *Perception as Bayesian inference*. Cambridge University Press.

Kruschke, J.K. (2015). *Doing Bayesian data analysis, Second Edition: A tutorial with R, JAGS, and Stan*. Burlington, MA: Academic Press

Luck, S. J., Woodman, G. F., & Vogel, E. K. (2000). Event-related potential studies of attention. *Trends in Cognitive Sciences, 4*(11), 432-440.

Ma, W. J., Beck, J. M., Latham, P. E., & Pouget, A. (2006). Bayesian inference with probabilistic population codes. *Nature Neuroscience, 9*(11), 1432-1438.

Myers, N. E., Stokes, M. G., & Nobre, A. C. (2017). Prioritizing information during working memory: Beyond sustained internal attention. *Trends in Cognitive Sciences, 21*(6), 449-461.

Nobre, A. C. (2022). Opening questions in visual working memory. *Journal of Cognitive Neuroscience*, 35(1), 49-59.

Nobre, A. C., & Stokes, M. G. (2019). Premembering experience: A hierarchy of time-scales for proactive attention. *Neuron, 104*(1), 132-146.

Oberauer, K., Stoneking, C., Wabersich, D., & Lin, H. Y. (2017). Hierarchical Bayesian measurement models for continuous reproduction of visual features from working memory. *Journal of Vision, 17*(5), 1-27.

Olivers, C. N., Meijer, F., & Theeuwes, J. (2006). Feature-based memory-driven attentional capture: visual working memory content affects visual attention. *Journal of Experimental Psychology: Human Perception and Performance, 32*(5), 1243-1265.

Park, H. B. (2025). Process dynamics of serial biases in visual perception and working memory processes. *Psychonomic Bulletin & Review*, Advance online publication.

Park, H., & Zhang, W. (2024). The dynamics of attentional guidance by working memory contents. *Cognition, 242*, 105638.

Park, H., & Zhang, W. (2022). Trial-by-trial mouse trajectory predicts variance in precision across working memory representations: A critical reanalysis of Hao et al. (2021). *Psychonomic Bulletin & Review, 29*(6), 2181-2191.

Park, H. B., Zhang, W., & Hyun, J. S. (2017). The aftermath of memory retrieval for recycling visual working memory representations. *Attention, Perception, & Psychophysics, 79*(5), 1393-1407.

Rademaker, R. L., Chunharas, C., & Serences, J. T. (2019). Coexisting representations of sensory and mnemonic information in human visual cortex. *Nature Neuroscience, 22*(8), 1336-1344.

Serences, J. T., Ester, E. F., Vogel, E. K., & Awh, E. (2009). Stimulus-specific delay activity in human primary visual cortex. *Psychological Science, 20*(2), 207-214.

Serences, J. T., & Yantis, S. (2006). Selective visual attention and perceptual coherence. *Trends in Cognitive Sciences, 10*(1), 38-45.

Shiffrin, R. M., Lee, M. D., Kim, W., & Wagenmakers, E. J. (2008). A survey of model evaluation approaches with a tutorial on hierarchical Bayesian methods. *Cognitive Science, 32*(8), 1248-1284.

Soto, D., Hodsoll, J., Rotshtein, P., & Humphreys, G. W. (2008). Automatic guidance of attention from working memory. *Trends in Cognitive Sciences, 12*(9), 342-348.

Summerfield, C., & De Lange, F. P. (2014). Expectation in perceptual decision making: Neural and computational mechanisms. *Nature Reviews Neuroscience, 15*(11), 745-756.

Tan, J., Zhao, Y., Wu, S., Wang, L., Hitchman, G., Tian, X., ... & Chen, A. (2014). The temporal dynamics of visual working memory guidance of selective attention. *Frontiers in Behavioral Neuroscience, 8*, 345.

Teng, C., Kaplan, S. M., Shomstein, S., & Kravitz, D. J. (2023). Assessing the interaction between working memory and perception through time. *Attention, Perception, & Psychophysics, 85*(7), 2196-2209.

Teng, C., & Kravitz, D. J. (2019). Visual working memory directly alters perception. *Nature Human Behaviour, 3*(8), 827-836.

Theeuwes, J., Olivers, C. N., & Chizk, C. L. (2005). Remembering a location makes the eyes curve away. *Psychological Science, 16*(3), 196-199.

van Loon, A. M., Olmos-Solis, K., Fahrenfort, J. J., & Olivers, C. N. (2018). Current and future goals are represented in opposite patterns in object-selective cortex. *eLife, 7*, e38677.

Wimmer, K., Nykamp, D. Q., Constantinidis, C., & Compte, A. (2014). Bump attractor dynamics in prefrontal cortex explains behavioral precision in spatial working memory. *Nature Neuroscience, 17*(3), 431-439.

Wolfe, J. M. (1994). Guided search 2.0 a revised model of visual search. *Psychonomic Bulletin & Review, 1*(2), 202-238.

Won, B. Y., & Zhang, W. (2025). Search strategy modulates memory-driven capture. *Attention, Perception, & Psychophysics*, Advance online publication.

Won, B., Park, H., & Zhang, W. (2023). Familiarity enhances mnemonic precision but impairs mnemonic accuracy in visual working memory. *Psychonomic Bulletin & Review, 30*. 1452-1462.

Zhang, W., & Luck, S. J. (2008). Discrete fixed-resolution representations in visual working memory. *Nature, 453*(7192), 233-235.

Table 1

Distinct Temporal and Mechanistic Components of Working Memory's Top-Down Influence

Component	Attentional Capture	Representational Shift
Cognitive Function	Attentional guidance, transient priority signal	Bias in perceptual/mnemonic decisions, evidence integration
Behavioral Signature	Endpoint-inconsistent trajectory curvature ($AUC_{capture}$)	Endpoint-consistent trajectory curvature (AUC_{shift}), final response bias
Temporal Dynamics	Fast; peaks early in movement and decays rapidly	Slow; emerges gradually and remains elevated throughout movement
Key Correlate	Movement onset latency	Magnitude of final response bias
Task Expression	Robust in WM → Perception (prospective template); minimal in Perception → WM	Present in both WM ↔ Perception (bidirectional)
Putative Mechanisms	Biased competition, top-down priority signaling from active WM templates	Bayesian integration, predictive coding (WM as priors)